

Title	FES-related tyrosine kinase activates the insulin-like growth factor-1 receptor at sites of cell adhesion
Authors	Stanicka, Joanna;Rieger, Leonie;O'Shea, Sandra;Cox, Orla T.;Coleman, Michael;O'Flanagan, Ciara;Addario, Barbara;McCabe, Nuala;Kennedy, Richard;O'Connor, Rosemary
Publication date	2018-03-15
Original Citation	Stanicka, J., Rieger, L., O'Shea, S., Cox, O., Coleman, M., O'Flanagan, C., Addario, B., McCabe, N., Kennedy, R. and O'Connor, R. (2018) 'FES-related tyrosine kinase activates the insulin-like growth factor-1 receptor at sites of cell adhesion', <i>Oncogene</i> , 37(23), pp. 3131-3150. doi: 10.1038/s41388-017-0113-z
Type of publication	Article (peer-reviewed)
Link to publisher's version	<a href="https://www.nature.com/articles/s41388-017-0113-z">https://www.nature.com/articles/s41388-017-0113-z</a> - 10.1038/s41388-017-0113-z
Rights	© Macmillan Publishers Limited, part of Springer Nature 2018
Download date	2024-05-15 07:24:36
Item downloaded from	<a href="https://hdl.handle.net/10468/7082">https://hdl.handle.net/10468/7082</a>

**FES-related Tyrosine Kinase activates the Insulin-like Growth Factor 1 Receptor at sites of cell adhesion**

<sup>1</sup>Joanna Stanicka, <sup>1</sup>Leonie Rieger, <sup>1</sup>Sandra O'Shea, <sup>1</sup>Orla Cox, <sup>1</sup>Michael Coleman, <sup>1</sup>Ciara O'Flanagan, <sup>1</sup>Janina Berghoff, <sup>1</sup>Barbara Addario, <sup>1</sup>Fionola Fogarty, <sup>2</sup>Nuala McCabe  
<sup>2</sup>Richard Kennedy, and \*<sup>1</sup>Rosemary O'Connor

<sup>1</sup>Cell Biology Laboratory, School of Biochemistry and Cell Biology, University College Cork, Cork, Ireland, and <sup>2</sup>Centre for Cancer Research and Cell Biology and Almac Diagnostics, Queens University Belfast, Northern Ireland

\*To whom correspondence should be addressed: [r.oconnor@ucc.ie](mailto:r.oconnor@ucc.ie)

**Running Title:** FER activates the IGF-1 Receptor at sites of cell adhesion

**Abstract:**

IGF-1 Receptor and Integrin cooperative signaling promotes cancer cell survival, proliferation and motility, but whether this influences cancer progression and therapy responses is largely unknown. Here we investigated the non-receptor tyrosine adhesion kinase FER, following its identification as a potential mediator of sensitivity to IGF-1R kinase inhibition in a functional siRNA screen. We found that FER and the IGF-1R co-locate in cells and can be co-immunoprecipitated. Ectopic FER expression strongly enhanced IGF-1R expression and phosphorylation on tyrosines 950 and 1131. FER phosphorylated these sites in an IGF-1R kinase-independent manner and also enhanced IGF-1-mediated phosphorylation of SHC, and activation of either AKT or MAPK signaling pathways in different cells. The IGF-1R,  $\beta$ 1 Integrin, FER and its substrate cortactin were all observed to co-locate in cell adhesion complexes, the disruption of which reduced IGF-1R expression and activity. High FER expression correlates with phosphorylation of SHC in breast cancer cell lines and with a poor prognosis in patient cohorts. FER and SHC phosphorylation and IGF-1R expression could be suppressed with a known ALK inhibitor (AP26113) that shows high specificity for FER kinase. Overall, we conclude that FER-enhances IGF-1R expression, phosphorylation and signaling to promote cooperative growth and adhesion signaling that may facilitate cancer progression.

## Introduction

The Insulin-like Growth Factor-1 Receptor (IGF-1R) and its signaling pathway has a well described function in sustaining a transformed phenotype [1-4]. *Igf-1r* knockout (*Igf-1r*<sup>-/-</sup>) mouse derived fibroblasts are refractory to transformation by oncogenes [3]. The phosphorylated receptor recruits IRS-1, IRS-2, or SHC to activate signaling pathways that promote cell survival, proliferation, or motility [1, 5]. However, despite compelling evidence for IGF-1R activity in facilitating cancer progression, efforts to target the IGF-1R in cancer have resulted in poor efficacy and clinical response [2, 6, 7]. Many reasons have been proposed for this, including observations that expression of IGF ligands and IGF-1R may not always correlate with signaling activity [7-10]. This has confounded the identification of useful biomarkers for IGF-1R activity inhibition in cancer cells.

Others and we have previously established that IGF-1R kinase activity and signaling output are modulated by adhesion-associated protein complexes [2, 5, 11]. This crosstalk contributes to the mitogenic, migratory and invasive phenotype of breast, lung, cervical and prostate cancer [11-14]. Indeed,  $\beta$ 1 Integrin ligation enhances IGF-1R surface expression and localization to sites of focal adhesion in prostate cancer cells [11]. A complex of IGF-1R-with  $\beta$ 1 Integrin that includes the scaffolding protein RACK1 and focal adhesion kinase, promotes MAPK pathway activity [5, 15]. Furthermore, adhesion-activated kinases SRC and FAK can directly phosphorylate IGF-1R *in vitro* and enhance IGF-1R-induced invasiveness of breast cancer cells [12, 14, 16, 17]. All of these observations indicate that the recruitment of the IGF-1R to adhesion complexes can significantly modify IGF-1R activation and signaling. However, it is not known whether adhesion signals are essential for IGF-1R activity in cancer progression or therapy responses.

We addressed this question by screening for proteins that modulate the cytotoxic response to IGF-1R tyrosine kinase inhibition using a functional siRNA screen [18]. We identified the non-receptor tyrosine FES-related (FER) kinase as a mediator of sensitivity to the IGF-1R tyrosine kinase inhibitor, BMS-754807, in MCF-7 cells. FER, along with FES, belongs to a distinct subfamily of receptor tyrosine kinases that possess FES/CIP4 homology **Bin-Amphiphysin-Rvs** (F-BAR) domains [19]. FER activity has been described in several cancers, including lung, hepatic, prostate and breast and is reported to facilitate tumorigenesis and chemoresistance by enhancing cell migration, invasion and proliferation [20-23]. FER has been

shown to interact with the EGFR, PDGFR, FLT3 and c-MET [21, 24-26] and proposed to facilitate crosstalk between growth factor receptors and cell-cell- or cell-matrix- adhesion complexes [19].

In this study we investigated whether FER modulates IGF-1R signaling in different cell lines. We found that FER associates with and enhances IGF-1R expression and activity at the plasma membrane and sites of cell adhesion. FER significantly increases IGF-1R phosphorylation on key tyrosines to enhance IGF-1-mediated activation of SHC and MAPK pathways in an adhesion-dependent manner. We conclude that FER kinase is an important modulator of IGF-1R activity in cancer cells. This may be particularly important in mesenchymal or migratory cancer cells where cooperative growth factor and adhesion signaling could facilitate cancer progression.

## **Results**

### **FER associates with and enhances IGF-1R expression levels.**

We identified FER as a modifier of responses to IGF-1R kinase inhibition in an siRNA screen [18] which suggested that FER may modulate IGF-1R activity. A previous study using peptide libraries identified FER as a kinase that could phosphorylate specific tyrosines in the Insulin and IGF-1 Receptors [27]. Both of these observations suggested that FER could modulate IGF-1R activity. To investigate this we first tested whether FER and the IGF-1R interact. Using proximity ligation assays (PLA) with anti-FER and IGF-1R antibodies, we observed that FER and IGF-1R are clearly found in proximity in MCF-7 cells (Fig. 1A). FER could also be co-immunoprecipitated with the IGF-1R from R<sup>+</sup> cells (mouse embryonic fibroblasts (MEFs) derived from *igf-1r*<sup>-/-</sup> mouse with IGF-1R re-expressed) (Fig. 1B). This was evident in cells that were serum deprived or stimulated with IGF-1, and in the presence of an IGF-1R kinase inhibitor BMS-754807 that suppressed IGF-1R autophosphorylation and IGF-induced activation of AKT (Fig 1B bottom panel). The IGF-1R and FER could also be co-immunoprecipitated from HEK293T cells that were co-transfected with IGF-1R and either wild type FER (WT), kinase-inactive FER (KD), or a SH2 domain mutant of FER (R483Q) (Fig. 1C). Interestingly, in these experiments it was noted that levels of IGF-1R expression were apparently higher in cells transfected with FER than in vector-expressing controls.

We further tested the effects of FER on IGF-1R expression in HEK293T cells. Co-transfection of plasmids encoding FER and the IGF-1R resulted in a 6-fold increase in IGF-1R protein levels compared to levels in cells transfected with IGF-1R and vector controls (Fig. 1D). This increase in protein was not due to enhanced transcription because *Igf-1r* mRNA expression levels were lower in cells expressing FER than in controls (Fig. 1E).

To test whether FER kinase activity was required to enhance IGF-1R protein levels, we transiently expressed IGF-1R in the presence of either FER/WT or FER/KD in HEK293T cells. Both FER/WT and FER/KD enhanced IGF-1R protein levels (Fig. 1F). Furthermore, levels of both IGF-1R/WT and kinase-dead IGF-1R (IGF-1R/KD) could be increased by co-transfection with FER (Fig. 1G). Taken together, these data indicate that FER and IGF-1R associate in different cells, and that FER enhance IGF-1R protein expression and steady state levels in a manner that is not dependent on either IGF-1R or FER kinase activity.

### **FER enhances phosphorylation of the IGF-1R and its signaling output.**

We next investigated whether FER influences IGF-1R phosphorylation and kinase activity by co-expressing FER with either IGF-1R/WT or IGF-1R/KD in HEK293T cells. We observed that FER expression specifically enhanced phosphorylation on Y950 (in the juxtamembrane region) and on Y1131 (in the kinase activation loop) on both IGF-1R/WT and IGF-1R/KD (Fig. 2A). Thus, IGF-1R kinase activity is not necessary for FER-enhanced phosphorylation of the Y950 and Y1131 sites. Phosphorylation of Y1135/1136 site in the kinase activation loop was evident with IGF-1R/WT, in the presence of FER, but not with kinase-inactive IGF-1R/KD (Fig. 2A), indicating that phosphorylation on this site is dependent on IGF-1R activity.

To exclude the possibility that the effects of FER on phosphorylation of IGF-1R/KD were due to endogenous, albeit low, levels of IGF-1R expression in HEK293T cells, we carried out similar experiments in R- cells. We observed that co-expression of FER with IGF-1R WT or KD also enhanced phosphorylation on Y950 and Y1131. Again, FER did not enhance phosphorylation on the Y1135/1136 site in IGF-1R/KD (Fig. 2B). To test whether enhanced phosphorylation of the IGF-1R by FER required FER kinase activity, we co-expressed the IGF-1R/WT or IGF-1R/KD with either FER or FER/KD. These experiments demonstrated that enhanced phosphorylation of IGF-1R (WT or KD) on Y950 and Y1131 was observed in both

serum-starved and IGF-1-stimulated cells. This was entirely dependent on an active FER kinase because the kinase inactive FER/KD did not enhance IGF-1R phosphorylation (Fig. 2C).

Since FER enhances phosphorylation of the IGF-1R independently of IGF-1R kinase activity, we next asked whether this phosphorylation enhances IGF-1 signaling responses. Ectopic FER expression in HEK293T cells did not alter IGF-1-stimulated activation of the PI3-K pathway activation, as measured by phosphorylation of AKT on S473 (Fig. 2D). This is likely due to the high basal levels of AKT phosphorylation present in HEK293T cells that are not reduced by serum starvation, resulting in no further response to IGF-1 stimulation. However, basal levels of SHC and FAK phosphorylation are low in these cells, which is consistent with their relatively weak adhesion to the substratum. Overexpression of FER/WT, but not FER/KD, significantly increased both basal and IGF-1-stimulated phosphorylation of SHC and ERK1/2 (Fig. 2D). Importantly, in vector control cells, IGF-1 did not induce detectable phosphorylation of Y239/240 on SHC, but IGF-1-induced phosphorylation on these sites was evident in the presence of FER expression. Phosphorylation of FAK (Y397 and Y925) and SRC (Y416) were also significantly enhanced by IGF-1 in FER/WT- but not in FER/KD-expressing cells (Fig. 2D).

Overall these data demonstrate that FER enhances phosphorylation of specific autophosphorylation sites on the IGF-1R, in a FER kinase-dependent but IGF-1R kinase-independent manner. This is associated with enhanced IGF-1 signaling responses.

### **FER, IGF-1R and $\beta$ 1 integrin associate in adhesion complexes that enhance FER activity**

The IGF-1R has previously been demonstrated to participate in a signaling complex with  $\beta$ 1 Integrin to promote cell proliferation and motility [5, 15]. FER has also been reported to regulate  $\beta$ 1 integrin signaling [28], so we hypothesized that FER is a component of a signaling complex containing Integrin and IGF-1R. In agreement with our observations in Figure 1 from PLA and immunoprecipitation, we observed that FER and IGF-1R strongly co-localize by co-immunofluorescence in MCF-7 cells (Fig. 3A). Furthermore, as shown by confocal microscopy the majority of surface IGF-1R in these cells is present at large complexes that also contain FER and  $\beta$ 1 Integrin (Fig. 3B) and vinculin (Fig. S1). These complexes represent sites of focal cell adhesion. In MDA-MB-231 cells FER and the IGF-1R were also both observed to co-localize with  $\beta$ 1 integrin at distinct sites of cell protrusion and adhesion (Fig. 3C).

We next asked whether an activated IGF-1R affects FER kinase activity, by measuring FER autophosphorylation on Y402 in HEK293T cells transfected with empty vector, IGF-1R/WT or IGF-1R/KD. IGF-1 strongly promoted FER autophosphorylation in vector-expressing cells, which indicates that activation of endogenous IGF-1R is sufficient to enhance FER activity. FER autophosphorylation was further increased in cells expressing IGF-1R/WT but not in cells expressing IGF-1R/KD (Fig. 3D), thus confirming a requirement for activated IGF-1R in FER activation. Overexpression of FER/WT but not KD in HEK293T cells increased the phosphorylation of SHC (P-Y239/240) and ERK1/2 (P-T202/T204); without any evident effect on phosphorylation of AKT (Fig. 3E). FER/WT also promoted a significant increase in phosphorylation of the focal adhesion-associated kinases SRC (Y416) and FAK (on both Y397 and Y925) (Fig. 3F).

Taken together these results demonstrate that FER and the IGF-1R are components of  $\beta$ 1 Integrin-anchored adhesion complexes that enhance activation and autophosphorylation of FER in an adhesion- and IGF-1- dependent manner. This suggests that the association of the IGF-1R with FER enhances cooperative IGF and adhesion signaling via the SHC, FAK and MAPK pathways and that these receptors may reciprocally activate each other.

### **FER suppression reduces IGF-1R expression and proliferation, and differentially affects cell migration.**

Having observed clear effects of FER on enhancing IGF-1R expression, phosphorylation and signaling we next asked whether suppression of FER would alter IGF-1R expression and activity. To do this we first screened a panel of siRNAs that specifically target FER in different breast cell lines (Fig. S2A). We observed a consistent suppression of FER with all siRNAs tested (except siFER4). IGF-1R expression levels were clearly reduced by most of these siRNAs in MCF-7, MDA-MB-231 cells and HS57T cells and MCF10A cells (Fig. S2A). To investigate this further we focused on two siRNAs (siFER2 which suppressed IGF-1R significantly and siFER3 which suppressed IGF-1R to a lesser extent) to further examine the effects of FER suppression on IGF-1R expression in all four cell lines. Both siFER2 and 3 substantially decreased IGF-1R protein levels at 48 hours post transfection in MCF-7, MDA-MB-231 and HS578T cells (Fig. 4A), while  $\beta$ 1 Integrins levels were largely unaffected (Fig. 4A and Fig.

S2B). Similar effects were observed for MCF10A cells at 48 hours (Fig. S2D) and for all cell lines at 72 hours post siRNA transfection (Fig. S2C and D).

We next investigated the effects of siFER2 and 3 on IGF-1 signaling in MCF-7 and MDA-MB-231 cells. In MCF-7 cells FER suppression had no effect on IGF-1-induced AKT phosphorylation, but both siRNAs clearly reduced IGF-1-stimulated phosphorylation of ERK1/2 (Fig. 4B). In MDA-MB-231 cells phosphorylation of ERK1/2 is generally not responsive to serum withdrawal or IGF-1, but IGF-1 induces strong phosphorylation of AKT. Here FER suppression with both siRNAs reduced IGF-1-induced phosphorylation of AKT (Fig. 4B). These data indicated that FER suppression can suppress IGF-1 signaling responses. In line with this we observed that cell proliferation rates in MCF-7 and MDA-MB-231 cell lines were suppressed by both siFER2 and siFER3 (Fig. 4C).

We next investigated the migratory potential of MDA-231 cells in Transwells with FER suppressed by siFER2 and siFER3. Surprisingly, we observed that siFER2 partially suppressed directional migration towards serum (approximately 30%) while siFER3 greatly impaired cell migration (by approximately 80%) (Fig. 4D). Interestingly, we noted that the morphology of cells transfected with either siFER2 or siFER3 was quite different (siFER2 caused cells to become more spread while siFER3 caused cells to become more spindle-like. These differences in morphology elicited by siFER2 and 3 were consistently and reproducibly observed in all cell lines transfected with these siRNAs (MCF-7, MDA-MB-231, HS578T and MCF10A cells) (Fig. S2E). MDA-MB-231 cell adhesion to fibronectin was impaired by siFER3, but not by siFER2 (Fig. 4E). Thus, our data show that similar levels of FER suppression can result in different effects on cell morphology and migratory potential. Although we cannot explain these consistently different siRNA effects the data suggest they may be related to suppressing FER function in the formation of dynamic cell adhesion structures, such as lamellipodia, that are necessary for cell migration.

Overall, we conclude that suppression of FER can reduce IGF-1R levels, IGF-1 signaling and cell proliferation. The data also indicate that similar suppression of FER does not correlate with similar effects on IGF-1R expression or cell phenotype, and FER suppression may result in different effects on cell morphology and migratory potential.

**Co-location of IGF-1R with FER in adhesion complexes enhances IGF-1R activity.**

Next, we sought to investigate whether FER is required for IGF-1R activity in adhesion complexes. First we investigated the effects of FER suppression with siFER2 and siFER3 on the association of IGF-1R and FER with  $\beta$ 1 Integrin in MDA-MB-231 cells. In agreement with our observations on cell morphology (Fig. S2E), we observed that cells transfected with siFER2 were more spread with fewer directional lamellipodia while cells transfected with siFER3 were elongated and spindle like (Fig. 5A and B). While IGF-1R could be observed to co-localize with  $\beta$ 1 integrin in adhesion complexes in control siNEG cells (Fig. 5A top panels), as described for Figure 3A and B, these structures and IGF-1R/ $\beta$ 1 Integrin co-localization were less evident in cells with FER suppressed (Fig 5A. B, C). As expected FER levels were suppressed by siFER2 and 3, and less association with  $\beta$ 1 Integrin was also observed (Fig. 5B). In MCF-7 cells transfected with siFER2, cell adhesion sites appeared to be smaller and less mature with considerably less vinculin  $\beta$ 1 integrin and IGF-1R present (Fig. S3A-C). These immature adhesion sites were especially evident by confocal imaging of siFER2-transfected cells that were stained for paxillin (Fig. S3B). Taken together these data indicate that suppression of FER with either siFER2 or siFER3 disrupts the formation of mature cell adhesions and functional lamellipodia necessary for directional cell migration.

Since siRNAs targeting FER apparently have different effects on cell morphology we also tested whether suppressing a well-described substrate of FER; cortical actin (cortactin, which has a role in both biosynthetic and recycling trafficking pathways [29-31]) had any effect on IGF-1R expression levels. We observed that the IGF-1R co-localizes with cortactin at sites of cell adhesion in MCF-7 cells (Fig. 5D). SiRNA-mediated suppression of cortactin reduced IGF-1R levels in both MCF-7 and MDA-MB-231 cells (Fig. 5E, F). This could be prevented by proteasome inhibition (shown for MDA-MB-231 cells in Fig. 5F).

To further test whether cell adhesion is required for FER-enhanced IGF-1R activity we compared the effects of FER on IGF-1R autophosphorylation and signaling in HEK293T cells that were adherent or maintained in suspension. We observed that the FER-enhanced phosphorylation of IGF-1R/WT and IGF-1R/KD on Y1131 was completely abolished when cells were not allowed to adhere (Fig. 5G). As expected, the phosphorylation of SHC and FAK, evident in adherent cells expressing IGF-1R/WT and FER/WT, was absent in non-adherent cells (Fig. 5G). Phosphorylation on the Y1135/1136 site was reduced by lack of adhesion, but in agreement with results in Figure 2, was not affected by FER. Interestingly, the effects of lack of

cell adhesion on IGF-1R were accompanied by a reduction in FER autophosphorylation (Fig. 5H). This demonstrates that adhesion signals enhance FER activity and its potentiation of IGF-1R and SHC/ERK1/2 phosphorylation.

These observations suggest that FER promotes the assembly of mature cell adhesions, which enhances the phosphorylation and activity of the IGF-1R.

**FER expression strongly correlates with EMT markers in Mesenchymal-like breast cancer, and its activity can be suppressed by an ALK kinase inhibitor.**

FER expression was previously associated with a poor outcome in Triple Negative Breast Cancer (TNBC) [28]. We explored whether this may be related to FER function in enhancing IGF-1R and adhesion signaling in breast cancer by first analyzing available datasets from breast tumors and cell lines. Kaplan-Meier survival plots derived from The Cancer Genome Atlas (TCGA) data [32] demonstrated that high expression of FER is associated with poor relapse free survival (RFS) among breast cancer patients ( $P=0.00015$ ;  $n=3951$ ; Fig. 6A, Fig. S4A). Following exclusion of systemically untreated patients, the hazard ratio (HR) rose to 1.63, while the median survival almost halved with high FER expression (65.1 to 34.82 months;  $P=0.91 \times 10^{-9}$ ; Fig. S4A). FER expression influences the survival of patients of Grade III, estrogen receptor (ER) negative and HER2 positive types of breast cancer (HR: 1.79;  $P=0.008$ ; median survival decrease from 47.52 to 27 months). Further analysis demonstrated that mesenchymal (M) and mesenchymal stem-like (MSL) were the subtypes most linked to high FER expression, with decreased median survival of MSL patients from 74 to 15.25 months (HR: 4.31;  $P=0.00028$ ; Fig. 6A). Cells of these subtypes have been described as less-differentiated and to manifest a highly migratory/invasive phenotype [33]. Interestingly, IGF-1R activity in tumors has also been associated with a mesenchymal and stem-like phenotype of cancer cells [7, 33].

In line with these observations, analysis of RNA-Seq expression profiles of 82 breast cancer cell lines extracted from the study of Marcotte *et al.* [34] demonstrated that migratory and mesenchymal breast cancer cell lines express FER at significantly higher levels than luminal cell lines ( $P<0.0001$ ; Fig. 6B, Fig. S4C). Expression of FER was also strongly correlated with expression of EMT markers, including *ZEB1/2*, *TWIST1/2*, *SNAI2 (SLUG)* and *VIM* (Pearson  $R \sim 0.4$ ,  $P<0.0003$ ; Fig. 6C, S9). We also investigated whether FER expression correlates with these markers in patient samples using TCGA) RNA-Seq data from 1215 breast cancer patients.

We found that FER expression strongly correlated with *ZEB1/2* (Pearson R: 0.6), *TWIST1* and *SNAI2* and other EMT markers (Fig. S4 B-E).

We also determined that FER expression in a panel of breast cancer cell lines could be positively correlated with phosphorylation of SHC (P-Y239/Y240) (Fig. 6D; S4F), noting that several of these cell lines expressed the p66 isoform of SHC that is associated with REDOX stress and more recently with coupling mechanical signals to activation of RhoA [35]. (The analysis of RNA sequencing (RNA-Seq) and reverse phase protein array (RPPA) data from 95 breast cancer patients, available from TCGA, further demonstrated a positive correlation in phosphorylation of SHC (P-Y317; Pearson R: 0.34; p=0.0008) and SRC (P-Y416; Pearson R: 0.27; p=0.007) and expression of FER (Fig. S4G).

All of the *in silico* analyses suggested an important function for FER in breast cancer aggressiveness. Therefore, we next sought to test the consequences of pharmacological inhibition of FER in breast cancer cells. As there is no specific FER kinase inhibitor available, we opted to test an inhibitor of the 2 anaplastic lymphoma kinase (ALK), AP26113 (Brigatinib). This compound potently inhibits FER in *in vitro* kinase assays and was described to have FER as its next most selective target following ALK [36]. A similar ALK inhibitor has been reported to inhibit FES kinase, which is structurally similar to FER [37] (Fig. S4H).

First, we tested AP26113 over a range of concentrations (50-500 nM) in HEK293T cells overexpressing FER (Fig. 6E). Concentrations as low as 50 nM, decreased FER autophosphorylation on Y412 by approximately 80% and also reduced FER-mediated phosphorylation of Y1131 in the IGF-1R. Consistent with our findings (Fig. 2) the inhibitor did not alter phosphorylation of Y1135/1136 in the IGF-1R (Fig 6E). Moreover, this kinase inhibitor suppressed phosphorylation of SHC and ERK1/2. This indicates that AP26113 inhibits FER kinase activity and FER-induced signaling.

We also tested AP26113 on breast cancers cells that express endogenous levels of FER. HS578T cells were chosen for these studies as a basal /mesenchymal-like/highly migratory breast cancer cell line with relatively high FER levels [38] (Fig 6D). Exposure of HS578T cells to AP26113 (100-200 nM) resulted in inhibition of FER kinase autophosphorylation (Fig. 6F). Interestingly, FER levels were also suppressed. This may be due to destabilization of inactive FER as was previously reported [30]. AP26113 also reduced phosphorylation of SHC, SRC and ERK1/2, without affecting AKT phosphorylation. Phosphorylation of the IGF-1R on Y950 and

1131 could not be detected in these cells probably because of the reduction in IGF-1R levels. We also asked whether AP26113 (0.5  $\mu$ M) altered the motility of HS578T cells over 15 hours in wound repair assays. We observed consistently impaired ability to fill the wound in the presence of AP26113 (Fig. 6G), and again, the drug reduced FER expression levels and phosphorylation, as well IGF-1R expression (Fig. 5H). Taken together, these data indicate that FER kinase activity and its actions in enhancing signaling pathways can be pharmacologically inhibited by the AP-26113 inhibitor. This inhibitor is currently being tested in phase 2 clinical trials as a therapy for non-small cell lung cancer (ID:NCT02706626).

### **Discussion:**

Cooperative IGF-1R and adhesion signaling has been proposed to facilitate cancer progression [2, 5, 39]. Here, we demonstrate that the non-receptor tyrosine kinase FER can regulate IGF-1R expression levels, activity, and adhesion-dependent signaling. FER has been reported to play a role in crosstalk between different receptor systems including cell-cell and cell-matrix complexes [19, 20]. Our findings (summarized in the model in Figure 7) indicate that FER acts as an important node in such crosstalk between Integrin and IGF-1R signaling and that FER can be reciprocally activated by both IGF-1 and adhesion signaling.

Here we show that FER and the IGF-1R strongly co-localize in cells, and interaction that does not require either FER or IGF-1R kinase activity. However, this interaction is essential for FER-enhanced IGF-1R phosphorylation and signaling. FER-induced phosphorylation of IGF-1R requires cell adhesion signals. It has been reported that FER regulates cellular distribution of Integrins by downregulating surface expression of  $\alpha$ 6 and  $\beta$ 1 Integrins [20]. Cooperation of growth factor receptors with different Integrin heterodimers may positively or negatively impact growth factor activation and signaling [40]. Hence, the modulation of surface expression of different Integrin subunits can alter the growth factor signal. FER could facilitate IGF-1R association with Integrin-adhesion complexes, thus enhancing its phosphorylation and signaling output. We observed that FER generally promotes autophosphorylation of adhesion-associated kinases, SRC and FAK, and these can, in turn, directly phosphorylate IGF-1R, when activated by Integrin-mediated cell adhesion.

While the role of FER in growth factor signaling has been previously documented [21, 22, 24], this is the first report of FER enhancing the expression levels and activity of the IGF-1R. FAK suppression has also been reported to decrease IGF-1R steady state levels [12, 16], again indicating that adhesion complexes support IGF-1R expression. The stability of other growth factor receptors can also be enhanced by adhesion complexes. For example, c-MET stability has been demonstrated to be dependent on Tensin 4, an adapter that links Integrins to  $\beta$  actin [41]. Therefore, we propose that the recruitment or localization of the IGF-1R to sites of cell adhesions results in enhanced IGF-1R stability. This could be mediated by the F-BAR domain of FER, because its oligomerization facilitates the formation of lamellipodia [42, 43]. We observed that suppression of cortactin, a substrate of FER, reduced IGF-1R steady state levels. Cortactin has been previously documented to prevent ligand-induced EGFR degradation and to enhance  $\beta$ 2 adrenergic receptor ( $\beta$ 2AR) recycling [29, 44]. On the other hand, FER suppression was reported to accelerate EGFR internalization [23]. Therefore, FER and adhesion-mediated stability of IGF-1R could be achieved by either decreased internalization, cortactin-mediated recycling, or decreased IGF-1R proteostasis during biosynthesis. It is possible that the effects of FER on enhancing IGF-1R expression through regulating proteostasis could be mediated by FER altering the glycosylation of the IGF-1R receptor, because FER has been demonstrated to regulate laminin-binding glycan [45]. Indeed, impaired regulation of IGF-1R proteostasis associated with loss of the tumour suppressor protein AIRAPL has recently been associated with myeloid cell transformation and leukemia [46]. The FES protein, which is closely related to FER, has also been associated with acute myeloid leukemia where it can be activated by FLT3 [18] to promote cell survival. It is interesting to speculate that FES may mediate some of its survival functions in myeloid leukemia by enhancing the expression or activity of the IGF-1R. This however remains to be tested.

An unexpected finding of our study was that siRNA-mediated suppression of FER using different oligonucleotides consistently reduced FER expression to apparently similar levels while causing consistently different effects on cell morphology and migratory potential. Our study and that of Ivanova *et al.* [20] analyzed FER suppression in the MDA-MB-231 breast cancer cell line, which displays a mesenchymal phenotype. We noted that FER suppression with siFER2 in our study produced a similar phenotype to that described by Ivanova *et al.*, with cells becoming more spread and less migratory. However, other siRNAs, in particular siFER3, which we also

studied in detail, produced different effects on cell morphology and migration. Interestingly, the different siRNAs produced consistently similar effects on cell morphology in different cell lines, which suggests they selectively target certain isoforms or complexes of FER. We could not establish whether different isoforms were implicated because we only observed changes in one protein with the available antibody. However, our data and previous reports on FER function in cell adhesion complexes indicate that the alterations in cell morphology elicited by siFER2 and siFER3 are both consistent with disrupting the formation of lamellipodia. One predicted outcome is that cells would become more spread cells with weak adhesions and lack of directional lamellipodia (observed with siFER2) and a second is that cells may not properly form lamellipodia (observed with siFER3). An additional possibility, suggested by the high levels of p66SHC observed in breast cancer cell lines that also express FER highly, is that p66SHC-mediated activation of the RhoA pathway in filopodia [35] may be affected by FER suppression. Overall, our observations illustrate that the use of selective siRNAs or shRNAs to investigate the physiological responses to FER suppression is not entirely straightforward.

A previous report demonstrated that FER expression is associated with aggressive breast cancer in patients (n=485) and inversely correlates with progression-free survival of ovarian cancer patients [24] [20]. Here, we analyzed a large subset of TCGA clinical survival data, which also shows that high FER expression (by RNA-Seq) correlates with poor relapse-free survival in breast cancer patients (n=3951). High expression of FER particularly increases the hazard ratio in the mesenchymal-subtype cohort of breast cancer patients (HR: 4.31). In support of this, we observed that mesenchymal/highly migratory breast cancer cells express FER at significantly higher level than their counterparts. Considering the strong effects of ectopic FER expression on IGF-1R phosphorylation, we propose that FER could mediate potentiation of IGF-1 signaling, particularly in cancers with an EMT or stem-like phenotype. This is consistent with the observation that IGF-1R expression and activation may be elevated in breast cancer stem cells [33]. IGF-1R activity has also been implicated in the self-renewal of lung adenocarcinoma and chemoresistant colon cancer stem cells [33], and may also facilitate the EMT transition of breast, colon, prostate and lung cancer cells [2, 12, 47, 48].

As described here and elsewhere, the role of FER in supporting an invasive phenotype highlights the need to develop specific FER kinase inhibitors. Our results lead us to propose that AP11236, which inhibits FER kinase and signaling at nanomolar concentration, is an

excellent candidate. AP1123 was developed as an anaplastic lymphoma kinase (ALK) inhibitor and is in clinical trials phase 2 for non-small cell lung cancer (Brigatinib; ID: NCT02706626). TAE684, a similar ALK-inhibitor has been reported recently to target FES that possesses a kinase domain highly homologous to FER [37]. Importantly, we observed that the residues required for interaction between TAE684 and FES kinase, that were identified by X-ray crystallography [37], are conserved in FER kinase. Inhibition of FER using AP26113 may present a useful therapeutic approach for mesenchymal-type breast cancers. In support of this concept, a tyrosine kinase inhibitor, PKC412 that was shown to specifically target a panel of post-EMT breast cancer cells mainly acts through inhibition of SYK and FER [49].

The ability of FER to mediate adhesion enhanced-phosphorylation of catalytically active or inactive IGF-1R, and IGF-1R in the presence of IGF-1R TKI (data not shown) could also provide a mechanistic explanation for the lack of efficacy of IGF-1R TKIs in the clinic. This conclusion is supported by reports that co-targeting the IGF-1R with SRC and FAK in breast, lung and pancreatic cancer models can synergistically decrease tumor growth [12, 14, 50]. Thus, co-targeting IGF-1R and adhesion signaling could improve the efficacy of IGF-1R inhibitors. We also propose that FER is a potential biomarker for adhesion-enhanced IGF-1R activity and its inhibition by AP26113 could effectively target tumor cells that are addicted to cooperative IGF-1R and adhesion signaling.

## **Materials and Methods**

### ***Cell culture and IGF-1 stimulation***

MCF-7, MDA-MB-231, MDA-MB-157, HEK293T, R-/IGF-1R/WT (+ 1.5  $\mu$ g/ml puromycin), Hs578T, R- and R+ cells were maintained in Dulbecco's Modified Eagles Medium (DMEM). MDA-MB-436 cells were cultured in a 50/50 mix of Leibovitz L15/RPMI media, and CAL51 cells in a 50/50 mix of DMEM/Hams Nutrient F12 media. HCC1806, ZR-75-1 and HCC70 cells were maintained in RPMI 1640. BT-549 cells were grown in RPMI 1640 with 0.023IU/ml Insulin. All media were supplemented with 10% (v/v) heat inactivated Fetal Bovine Serum (FBS), 10 mM L-Glutamine, and 5 mg/ml penicillin/streptomycin. MCF-10A cells were cultured as previously described [51]. Cells were cultured at 37 °C in a humidified atmosphere at 5% CO<sub>2</sub>. All cells were determined to be free of mycoplasma.

For analysis of non-adherent (suspension) cells, cells were plated in duplicate on 10cm plates and cultured overnight in complete medium. Cells from one plate of each cell type enzymatically detached for 5 min, and cells recovered by centrifugation (1000 RPM) for 5 min. Cells were then washed with PBS and resuspended in complete medium (10mls) in a 50ml tube with occasional rotation for a total of 4 h prior to harvesting for lysis.

For analysis of IGF-1 stimulation responses, cells were cultured at seeding densities that allowed for an approximate 70% confluency after 20 h. Cells were incubated in serum-free medium for 4 h prior to stimulation with 10ng/ml IGF-1 where appropriate. To terminate stimulation, cells were placed on ice and washed immediately with ice-cold PBS.

### ***Immunofluorescence and Proximity Ligation Assay and Microscopy***

Cells were seeded on serum-coated 10 mm glass coverslips, washed with phosphate-buffered saline, fixed with 4% paraformaldehyde in PHEM buffer for 30 min at 37 °C, quenched with 50 mM Ammonium Chloride for 15 min and permeabilized using 0.1% Triton/PHEM for 5 min. Cells were then blocked for 30 min using 5% donkey serum/PHEM, incubated for 1 h with the indicated primary antibodies diluted 1:100 (unless specifically stated otherwise in figure legends) in the blocking buffer and washed with PHEM buffer. This was followed by incubation with Alexa488- (1:200) or Cy3- (1:1000) conjugated secondary antibodies with Hoechst. For Duolink PLA (Sigma Aldrich) experiments, cells were fixed, quenched and permeabilized exactly in the same manner as for the standard immunofluorescence. Following this, cells were incubated with Duolink blocking buffer in a pre-heated humidity chamber for 30 min at +37 °C. Primary antibodies anti-IGF-1R (#3027 (1:200) or #9750 (1:100); Cell Signalling) and anti-FER (#4268 (1:200); Cell Signalling), were diluted in the Duolink blocking buffer and incubated on the cells in a humidity chamber overnight. PLA anti-rabbit plus and anti-mouse minus probes were used to label primary antibodies. The probes were mixed and diluted 1:5 in a blocking buffer. The slides are incubated the slides in a pre-heated humidity chamber for 1 h at +37 °C. The ligation stock (1:5) with ligase (1:40) was incubated on the coverslips in a pre-heated humidity chamber for 30 min at +37 °C. The amplification stock (1:5) with polymerase (1:80) was incubated on the coverslips in a pre-heated humidity chamber for 100 min at +37 °C. The solution was removed and coverslips dried at room temperature in the dark. Coverslips were

mounted onto the slides using a minimal volume of Duolink In Situ Mounting Medium with DAPI.

Images were acquired using a SPOT charge-coupled device camera mounted on a Nikon T600 fluorescent microscope (Kingston Upon Thames, UK). For confocal microscopy, images were acquired using a Flouview FV1000 confocal laser scanning microscope (numerical aperture:1.4) with a  $\times 60$  oil or  $\times 100$  oil immersion objective. Maximum intensity projections and z-stacks were processed and analyzed in Olympus Fluoview (FV10-ASW 4.0 Viewer) where brightness and contrast were adjusted.

### ***SDS–polyacrylamide gel electrophoresis and Western blotting***

Cellular protein extracts were prepared with a lysis buffer (NP-40 or RIPA; as described previously) for 30 min on ice [5]. Protein concentration was determined via Bradford Assay, and samples were then either denatured by boiling for 5 minutes in 5X loading buffer (2% w/v SDS, 8% v/v glycerol, 60 mM Tris-HCL, pH 6.8, 1.2%  $\beta$ -mercaptoethanol, and 0.2-0.4% Bromophenol Blue), or carried through to immunoprecipitation studies. Proteins were resolved by 4–20% SDS–polyacrylamide gel electrophoresis. Proteins were transferred to nitrocellulose membrane and blocked for 1 h at room temperature in 5% milk in Tris-buffered saline-T (20 mM Tris, 150 mM NaCl and 0.05% Tween 20, pH 7.6). Primary antibodies were diluted in 5% milk in Tris-buffered saline-T and incubated with membranes at 4 °C overnight. IRDYE-conjugated secondary antibodies were used for detection with the Odyssey Image Scanner System (LI-COR Biosciences) and the Odyssey quantification software. Where re-probes were necessary, membranes were incubated with stripping buffer (200 mM NaOH, 1 % SDS) for 20 min at room temperature. Membranes were then washed, blocked, and incubated with appropriate antibodies.

### ***Immunoprecipitation***

Cell lysates were pre-cleared using Protein G-Agarose beads with lysis buffer and inhibitors for 1 h at 4°C at a rotor speed of 5 RPM, and were then recovered by centrifugation at 3000 RPM for 3 min at 4°C. Primary antibodies were incubated at 4°C for 1 h. Immune complexes were obtained by adding 25  $\mu$ l of pre-washed Protein G-Agarose beads for 1 h at 4 °C, and then recovered by centrifugation at 1000 RPM for 3 min at 4 °C. Immunoprecipitates were washed three times with ice-cold lysis buffer followed by centrifugation. 2X loading buffer was added to

each sample prior to boiling for 5 min. Samples were separated by SDS-PAGE as described above.

### ***DNA Transfection and mutagenesis***

Cells were transiently transfected with pcDNA3 plasmids encoding WT or mutant IGF-1R (IGF-1R/KD: K1003R) and pSG5 plasmids encoding FER kinase or kinase-dead FER Kinase (D743R; KD) or SH2-domain mutant (R483Q; SH2). The corresponding empty vector was transfected for each plasmid as control. Mutagenesis of pSG5 plasmid to introduce D743R (FER/KD and R483Q (FER/SH2) was carried out using the QuikChange Lightning site-directed mutagenesis kit (Agilent, #210518).

For transfection of R- cells, cells were seeded at a density of  $1.5 \times 10^6$  cells/10 cm tissue culture dish, in antibiotic-free medium. Eighteen hours later, cells were transfected with relevant DNA (10  $\mu$ g) and Lipofectamine 2000 (diluted in OptiMem) per 10 cm tissue culture dish and then incubated at 37 °C overnight. Transfected R- cells were subsequently split in preparation for experiments to be carried out 48 h after transfection. MCF-7 and MDA-MB-231 cells were transfected in a similar manner to R- cells, except for: seeding at  $1.2 \times 10^6$  cells/10 cm and the use of Lipofectamine; For co-transfection of IGF-1R and FER in HEK 293-T cells; cells were transfected using Calcium Phosphate. Briefly, cells were seeded 5 h prior to transfection to give a confluency of 70%. 3  $\mu$ g of pSG5 encoding FER, together with 1  $\mu$ g of pcDNA3 IGF-1R expressing plasmids were added to CaCl<sub>2</sub>. The DNA/ CaCl<sub>2</sub> mixture was then added dropwise to 2X HBSS at a ratio of 1:1. Samples were allowed to stand for 1-2 min after which the solution was distributed to the pre-seeded cells in a dropwise manner. Cells were then incubated overnight to allow the transfection to proceed, after which cells were reseeded for experimental purposes and lysed 24 h later.

### ***siRNA Transfection***

A non-targeting oligonucleotide, Silencer Negative siRNA Control #2 (AM4311) from Ambion (Cambridgeshire, UK) was used as a Negative Control. Individual oligos targeting human FER kinase: siFER2 (S100287756; CAGATAGATCCTAGTACAGAA) and siFER3 (S102622067; CAGAACAACCTTAGTAGGATAA) were obtained from Qiagen. Sequences for the other FER siRNAs from Qiagen tested are listed in Supplementary Table 1, as well as those of the

SMARTpool ON-TARGETplus FER siRNA (L-003129-00-0005), which was purchased from Dharmacon. Transfections were performed using a final concentration of 20 nM siRNA, except where otherwise noted, using RNAiMAX, according to the manufacturer's recommendations. Briefly, cells were trypsinized and re-suspended in antibiotic-free culture media with serum. siRNA oligonucleotides were diluted in OptiMem media. RNAiMAX transfection reagent was added to the siRNA solutions. siRNA/RNAiMAX complex was pipetted to 6-well plate and  $6.5 \times 10^5$  cells per well were then added. Cells were allowed to adhere overnight to the tissue culture plate. 24 h post-transfection, the siRNA/RNAiMAX complex was removed and cells were reseeded for experiments.

### ***Cell Proliferation, Migration and Adhesion Assays***

*Proliferation:* Cells were transfected as described above and replated in triplicates 24 h post-transfection, at a density of to  $3.0 \times 10^4$  cells/well of a 24 well plate. Cells were collected every 24 h after replating, up to 96 h. Media was removed, cells were washed once with PBS and fixed with 96% Ethanol for 10 mins, followed by staining with 0.05% crystal violet in 20% Ethanol for 30 min. Crystal violet staining of the cells was assessed by infrared scanning using Odyssey Scanner and quantified using Licor Image studio Lite software (LI-COR Biosciences).

*Migration; Wound-Healing assay:* A scratch-wound healing assay was used to assess migration of cells following the treatment with FER-i (AP26113). HS578T cells were seeded in six-well plates at a concentration of  $3.5 \times 10^5$  cells/ml 24 h prior to wounding. The monolayer was scratched using a sterile P10 tip (Time 0 h). AP26113 was added to the cells, while DMSO at the appropriate volume was added to the control cells. Cells were allowed to migrate for 15 h. Pictures of cells were captured using a 10x objective at Time 0h and 15 h.

*Migration; Transwell Assay:* Migration assays were performed using 6.5mm transwell inserts with 8.0  $\mu$ m membrane (costar#3422; Cambridge, MA), according to the manufacturer's recommendations. Briefly, 24 hr post-transfection with siNEG, siFER2 or siFER3 siRNAs,  $2 \times 10^5$  MDA-MB-231 cells were seeded onto the upper part of the transwell chamber in serum-free medium, and allowed to migrate towards 10% serum in the lower well of the chamber for 24hr. Cells were also added to 2 additional wells without transwells to serve as cell proliferation controls. These controls, cells that had migrated to the underside of the transwell membrane ('Membrane'), and cells that had migrated through the membrane entirely and attached to the

bottom of the well ('Through migration') were fixed and stained with 0.05% crystal violet and measured using an Odyssey scanner quantified using Licor Image studio Lite software (LI-COR Biosciences).

*Adhesion assay:* The wells of a 96-well plate were coated with 100 µl of fibronectin (Sigma, UK; 5 µg/ml) or collagen I (Gibco, Lifetechnologies, Grand Island, NY; 10 µg/ml) for 2 h at 37°C. The plates were washed extensively with PBS and blocked with 100 µl of 2.5% bovine serum albumin/well for 1 h before further washing with PBS. Cells (100 µl containing  $5 \times 10^4$  cells) were added to each coated well in triplicate and allowed to attach for the indicated times. The medium was removed, the wells were washed with PBS, and attached cells were fixed with Methanol and stained with 0.05% Crystal Violet, scanned and quantified as described above.

### ***RNA isolation and quantitative RT-PCR***

Total RNA was isolated using the Trizol method and cDNA synthesis was carried out by reverse transcription with equal amounts of RNA (2 µg) using a cDNA synthesis kit (Invitrogen).

Quantitative PCR was carried out using the LightCycler instrument; Roche Molecular Biochemicals (East Sussex, UK) with QuantiTect SYBR Green technology (Qiagen, Crawley, West Sussex, UK) using the following primers: 1) IGF-1R: Forward: 5'-

ATGTCCAGGCCAAAACAGGAT-3'; Reverse: 5'-CCTCCCCTCATCAGGAACG-3' 2)

FER: Forward: 5'-GCTTCAGAAACGGCCATCAC-3'; Reverse: 5'-

AGCGTCTCCATGATGAGGTG-3'. The delta-delta CT method was used to analyze data and determine relative mRNA expression levels

### ***Bioinformatic analysis***

TCGA RNA-Seq data (n=1215) was accessed from the MD-Anderson Standardised data browser ([bioinformatics.mdanderson.org/cancer/databrowser/](http://bioinformatics.mdanderson.org/cancer/databrowser/)). Correlation of gene expression was calculated using Pearson's product moment correlation coefficient (r), statistical significance was determined using a modified t test (p).

To determine correlation between protein levels and RNA levels in breast cancer, an RPPA dataset was downloaded, TCGA patient sample ID's were then aligned to the RNA-Seq matrix to ensure each pair corresponded to two different assays conducted on the same primary sample. Correlation was then calculated as for RNA-Seq analysis (n=95).RNA-Seq data for an extended

panel of breast cancer cell lines was obtained from the supplementary material of Marcotte *et al.* [34].

### ***Kaplan-Meier (KM) Plotter Analysis***

The KM Plotter online survival analysis was used to generate Kaplan Meier plots (Szasz *et al.*, 2010). Gene expression data and relapse free and overall survival information are downloaded from GEO (Gene Expression Omnibus; Affymetrix microarrays only), EGA and TCGA. Patient samples were split into two groups according to median expression of FER (ID: 206412). The two patient cohorts are compared by a Kaplan-Meier survival plot, and the hazard ratio with 95% confidence intervals, median survival and logrank P value are calculated.

### ***Statistical Analysis and Densitometry***

Densitometry of Western blots was carried out by measuring the intensity of immunolabelled protein bands using Odyssey/Image Studio Light Software. Results were expressed as ratio of phospho:total protein, or where relevant as ratios to total loading controls. In order to thoroughly and simultaneously investigate several IGF-1R phosphorylation sites, and FER/phospho-FER levels, technical replicates of lysates were run in parallel on the same or separate blots. To ensure consistent protein loading, each blot was probed with a loading control (e.g. actin, tubulin, GAPDH or pan-signalling proteins such as AKT, ERK1/2 or SHC), one of which was included in each figure dataset as a representative of protein loading for those samples. For data analysis of protein expression however, the respective protein loading control for each sample on a particular blot was used for normalisation of protein expression. Changes in ratio of phospho/pan-protein levels were expressed as fold changes relative to the untreated control. Statistical significance was determined using Student-T-Test using Microsoft Excel or GraphPad Prism. Significance was classified as a P value of \* $<0.05$ , \*\* $<0.01$ , \*\*\* $<0.001$ . Where specified, One- or Two-way-Anova (GraphPad Prism) was used to determine significance, were a P value of  $<0.05$  was deemed significant. All graphs were produced using GraphPad Prism and are graphed using Standard Error of the Mean (SEM).

### **References:**

1. Samani, A.A., *et al.*, *The Role of the IGF System in Cancer Growth and Metastasis: Overview and Recent Insights*. Endocrine Reviews, 2007. **28**(1): p. 20-47.

2. Cox, O.T., et al., *IGF-1 Receptor and Adhesion Signaling: An Important Axis in Determining Cancer Cell Phenotype and Therapy Resistance*. Front Endocrinol (Lausanne), 2015. **6**: p. 106.
3. Baserga, R., F. Peruzzi, and K. Reiss, *The IGF-1 receptor in cancer biology*. Int J Cancer, 2003. **107**(6): p. 873-7.
4. Pollak, M., *The insulin and insulin-like growth factor receptor family in neoplasia: an update*. Nat Rev Cancer, 2012. **12**(3): p. 159-69.
5. Kiely, P.A., et al., *RACK1-mediated integration of adhesion and insulin-like growth factor I (IGF-I) signaling and cell migration are defective in cells expressing an IGF-I receptor mutated at tyrosines 1250 and 1251*. J Biol Chem, 2005. **280**(9): p. 7624-33.
6. King, H., et al., *Can we unlock the potential of IGF-1R inhibition in cancer therapy?* Cancer Treat Rev, 2014. **40**(9): p. 1096-105.
7. Farabaugh, S.M., D.N. Boone, and A.V. Lee, *Role of IGF1R in Breast Cancer Subtypes, Stemness, and Lineage Differentiation*. Front Endocrinol (Lausanne), 2015. **6**.
8. Niepel, M., et al., *Profiles of Basal and stimulated receptor signaling networks predict drug response in breast cancer lines*. Sci Signal, 2013. **6**(294): p. ra84.
9. Kostler, W.J., et al., *Insulin-like growth factor-1 receptor (IGF-1R) expression does not predict for resistance to trastuzumab-based treatment in patients with Her-2/neu overexpressing metastatic breast cancer*. J Cancer Res Clin Oncol, 2006. **132**(1): p. 9-18.
10. Law, J.H., et al., *Phosphorylated Insulin-Like Growth Factor-I/Insulin Receptor Is Present in All Breast Cancer Subtypes and Is Related to Poor Survival*. Cancer Research, 2008. **68**(24): p. 10238-10246.
11. Goel, H.L., et al., *beta1A integrin expression is required for type I insulin-like growth factor receptor mitogenic and transforming activities and localization to focal contacts*. Cancer Res, 2005. **65**(15): p. 6692-700.
12. Taliaferro-Smith, L., et al., *FAK activation is required for IGF1R-mediated regulation of EMT, migration, and invasion in mesenchymal triple negative breast cancer cells*. Oncotarget, 2015. **6**(7): p. 4757-72.
13. Shen, M.R., et al., *Insulin-like growth factor 1 is a potent stimulator of cervical cancer cell invasiveness and proliferation that is modulated by alphavbeta3 integrin signaling*. Carcinogenesis, 2006. **27**(5): p. 962-71.
14. Min, H.Y., et al., *Targeting the insulin-like growth factor receptor and Src signaling network for the treatment of non-small cell lung cancer*. Mol Cancer, 2015. **14**.
15. Hermanto, U., et al., *RACK1, an Insulin-Like Growth Factor I (IGF-I) Receptor-Interacting Protein, Modulates IGF-I-Dependent Integrin Signaling and Promotes Cell Spreading and Contact with Extracellular Matrix*. Molecular and Cellular Biology, 2002. **22**(7): p. 2345-2365.
16. Andersson, S., et al., *Focal adhesion kinase (FAK) activates and stabilizes IGF-1 receptor*. Biochem Biophys Res Commun, 2009. **387**(1): p. 36-41.
17. Peterson, J.E., et al., *Src phosphorylates the insulin-like growth factor type I receptor on the autophosphorylation sites. Requirement for transformation by src*. J Biol Chem, 1996. **271**(49): p. 31562-71.
18. O'Flanagan, C.H., et al., *IGF-1R inhibition sensitizes breast cancer cells to ATM-related kinase (ATR) inhibitor and cisplatin*. Oncotarget, 2016. **7**(35): p. 56826-56841.
19. Greer, P., *Closing in on the biological functions of fps/fes and fer*. Nat Rev Mol Cell Biol, 2002. **3**(4): p. 278-289.

20. Ivanova, I.A., et al., *FER kinase promotes breast cancer metastasis by regulating [alpha]6- and [beta]1-integrin-dependent cell adhesion and anoikis resistance*. *Oncogene*, 2013. **32**(50): p. 5582-5592.
21. Guo, C. and G.R. Stark, *FER tyrosine kinase (FER) overexpression mediates resistance to quinacrine through EGF-dependent activation of NF-kappaB*. *Proc Natl Acad Sci U S A*, 2011. **108**(19): p. 7968-73.
22. Ahn, J., et al., *Fer protein-tyrosine kinase promotes lung adenocarcinoma cell invasion and tumor metastasis*. *Mol Cancer Res*, 2013. **11**(8): p. 952-63.
23. Sangrar, W., et al., *Amplified Ras-MAPK signal states correlate with accelerated EGFR internalization, cytostasis and delayed HER2 tumor onset in Fer-deficient model systems*. *Oncogene*, 2015. **34**(31): p. 4109-4117.
24. Fan, G., et al., *HGF-independent regulation of MET and Gab1 through non-receptor tyrosine kinase FER (609.4)*. *The FASEB Journal*, 2014. **28**(1 Supplement).
25. Lennartsson, J., et al., *The Fer tyrosine kinase is important for platelet-derived growth factor-BB-induced signal transducer and activator of transcription 3 (STAT3) protein phosphorylation, colony formation in soft agar, and tumor growth in vivo*. *J Biol Chem*, 2013. **288**(22): p. 15736-44.
26. Voisset, E., et al., *FES kinases are required for oncogenic FLT3 signaling*. *Leukemia*, 2010. **24**.
27. Liu, B.A., et al., *SRC Homology 2 Domain Binding Sites in Insulin, IGF-1 and FGF receptor mediated signaling networks reveal an extensive potential interactome*. *Cell Commun Signal*, 2012. **10**(1): p. 27.
28. Ivanova, I.A., et al., *FER kinase promotes breast cancer metastasis by regulating alpha6- and beta1-integrin-dependent cell adhesion and anoikis resistance*. *Oncogene*, 2013. **32**(50): p. 5582-92.
29. Vistein, R. and M.A. Puthenveedu, *Src regulates sequence-dependent beta-2 adrenergic receptor recycling via cortactin phosphorylation*. *Traffic*, 2014. **15**(11): p. 1195-205.
30. Craig, A.W.B., et al., *Mice Devoid of Fer Protein-Tyrosine Kinase Activity Are Viable and Fertile but Display Reduced Cortactin Phosphorylation*. *Molecular and Cellular Biology*, 2001. **21**(2): p. 603-613.
31. Cao, H., et al., *Actin and Arp1-dependent recruitment of a cortactin-dynamain complex to the Golgi regulates post-Golgi transport*. *Nat Cell Biol*, 2005. **7**(5): p. 483-92.
32. Szasz, A.M., et al., *Cross-validation of survival associated biomarkers in gastric cancer using transcriptomic data of 1,065 patients*. *Oncotarget*, 2016. **7**(31): p. 49322-49333.
33. Malaguarnera, R. and A. Belfiore, *The Emerging Role of Insulin and Insulin-Like Growth Factor Signaling in Cancer Stem Cells*. *Front Endocrinol (Lausanne)*, 2014. **5**.
34. Marcotte, R., et al., *Functional Genomic Landscape of Human Breast Cancer Drivers, Vulnerabilities, and Resistance*. *Cell*, 2016. **164**(1-2): p. 293-309.
35. Wu, R.F., et al., *p66Shc couples mechanical signals to RhoA through FAK-dependent recruitment of p115-RhoGEF and GEF-H1*. *Mol Cell Biol*, 2016. **36**(22): p. 2824-2837.
36. Zhang, S., et al., *The Potent ALK Inhibitor Brigatinib (AP26113) Overcomes Mechanisms of Resistance to First- and Second-Generation ALK Inhibitors in Preclinical Models*. *Clin Cancer Res*, 2016. **22**(22): p. 5527-5538.
37. Hellwig, S., et al., *Small Molecule Inhibitors of the c-Fes Protein-tyrosine Kinase*. *Chem Biol*, 2012. **19**(4): p. 529-40.

38. Charafe-Jauffret, E., et al., *Gene expression profiling of breast cell lines identifies potential new basal markers*. *Oncogene*, 2006. **25**(15): p. 2273-84.
39. Zhang, W., et al., *RACK1 Recruits STAT3 Specifically to Insulin and Insulin-Like Growth Factor 1 Receptors for Activation, Which Is Important for Regulating Anchorage-Independent Growth*. *Molecular and Cellular Biology*, 2006. **26**(2): p. 413-424.
40. Ivaska, J. and J. Heino, *Cooperation between integrins and growth factor receptors in signaling and endocytosis*. *Annu Rev Cell Dev Biol*, 2011. **27**: p. 291-320.
41. Muharram, G., et al., *Tensin-4-Dependent MET Stabilization Is Essential for Survival and Proliferation in Carcinoma Cells*. *Dev Cell*, 2014. **29**(4): p. 421-36.
42. Oneyama, C., et al., *Fer tyrosine kinase oligomer mediates and amplifies Src-induced tumor progression*. *Oncogene*, 2016. **35**(4): p. 501-512.
43. Itoh, T., et al., *The Tyrosine Kinase Fer Is a Downstream Target of the PLD-PA Pathway that Regulates Cell Migration*. *Science Signaling*, 2009. **2**(87): p. ra52.
44. van Rossum, A., et al., *Cortactin overexpression results in sustained epidermal growth factor receptor signaling by preventing ligand-induced receptor degradation in human carcinoma cells*. *Breast Cancer Res*, 2005. **7**(6): p. 235-7.
45. Yoneyama, T., et al., *Fer kinase regulates cell migration through  $\alpha$ -dystroglycan glycosylation*. *Molecular Biology of the Cell*, 2012. **23**(5): p. 771-780.
46. Osorio, F.G., et al., *Loss of the proteostasis factor AIRAPL causes myeloid transformation by deregulating IGF-1 signaling*. *Nat Med*, 2016. **22**(1): p. 91-6.
47. Li, H., et al., *IGF-1R signaling in epithelial to mesenchymal transition and targeting IGF-1R therapy: overview and new insights*. *Mol Cancer*, 2017. **16**.
48. Graham, T.R., et al., *Insulin-like growth factor-1-dependent up-regulation of ZEB1 drives epithelial-to-mesenchymal transition in human prostate cancer cells*. *Cancer Res*, 2008. **68**(7): p. 2479-88.
49. Muellner, M.K., et al., *Targeting a cell state common to triple-negative breast cancers*. *Mol Syst Biol*, 2015. **11**(2).
50. Zheng, D., et al., *A Novel Strategy to Inhibit FAK and IGF-1R Decreases Growth of Pancreatic Cancer Xenografts*. *Mol Carcinog*, 2010. **49**(2): p. 200-9.
51. Deevi, R.K., O.T. Cox, and R. O'Connor, *Essential function for PDLIM2 in cell polarization in three-dimensional cultures by feedback regulation of the beta1-integrin-RhoA signaling axis*. *Neoplasia*, 2014. **16**(5): p. 422-31.

#### **Acknowledgements:**

We would like to acknowledge colleagues in the Cell Biology Laboratory and the Centre for Cell Biology and Cancer Research for helpful discussions.

**Funding:** This work was funded by a Science Foundation Ireland Principal Investigator award 11/PI/1139, and the European Union FP7 Marie Curie Industry-Academia Partnerships and Pathways (IAPP) Programme 251480 BiomarkerIGF.

**Author Contributions:** JS contributed to conception and design of experiments, acquisition and interpretation of data and drafting the manuscript. SOS contributed to design of experiments, analysis and interpretation of data. LR, MC, OTC, JB, COF, BA, FF, and NMcC contributed to

design of experiments, acquisition and analysis of data. RK contributed to conception of study and reviewing the manuscript. RO'C contributed to conception design, interpretation of data and drafting the article.

**Competing Interests:** The authors have no competing financial interests in relation to the work described.

## Figure Legends

### Figure 1.

#### **FER associates with IGF-1R and enhances expression levels.**

##### **A: Proximity ligation assay (PLA) showing protein interaction between FER and IGF-1R**

**in MCF-7 cells.** Cells were cultured on coverslips, fixed and probed with one of two rabbit anti-IGF-1R antibodies (#3027, top panels or #9750, bottom panels) and mouse anti-FER antibody (#4268), and then subjected to PLA as described in detail in the methods section. The negative controls are cells without primary antibody subjected to PLA. Slides were examined by confocal microscopy using a Zeiss LSM700 inverted confocal microscope equipped with 60x oil-immersion objective, numerical aperture 1.4. Z-projected images of the collected Z-stack were performed and analyzed using the Olympus Fluoview software. Each red spot represents a single interaction. The presented images are maximum intensity projections of Z-stacks acquired from a representative of three independent experiments.

**B: Western blot analysis of co-immunoprecipitated IGF-1R and FER.** The IGF-1R was immunoprecipitated from R+ cells that were serum-starved (-), stimulated with IGF-1 (10 min; 10 ng/ml; +), or stimulated with IGF-1 in the presence of BMS-754807 (BMS). Beads-and-lysates (B&L) and beads-and-antibody (B&A) controls were included as well as cell lysates from the immunoprecipitation inputs. Blots were probed with anti-IGF-1R and anti-FER antibodies. The panel underneath shows the levels of P-1135/1136 IGF-1R and P-AKT in total lysates used for immunoprecipitation (as controls for BMS-754807 inhibition of IGF-1R kinase activity).

##### **C: Western blot analysis of IGF-1R and FER co-immunoprecipitated from HEK293T cells.**

The IGF-1R was immunoprecipitated from cells that were transfected with plasmids encoding IGF-1R Wild Type (IGF-1R/WT (pcDNA3)), FER (WT (pSG5-FER)), FER/Kinase Dead (FER/KD; D743R mutant), an SH2-domain mutant of FER (R483Q; SH2), or corresponding empty vector plasmids (EV), 48 h post-transfection. Beads-and-lysates (B&L) and beads-and-antibody (B&A) controls were included as well as the immunoprecipitation inputs. The panel below shows the levels of FER and IGF-1R in the cell lysates used for immunoprecipitation.

**D, E: FER enhances IGF-1R protein expression levels.** HEK293T cells were co-transfected with empty vector (pcDNA3-EV; EV, x-axis on graph) or IGF-1R/WT (IGF-1R, x axis on graph) plus either empty vector (pSG5-EV; EV, black bars on graph) or FER/WT (FER, grey bars on graph), 48 h post-transfection. Cells were lysed and immunoblotted for IGF-1R and FER

expression with  $\beta$  actin as a loading control (D). Or mRNA expression of *igf-1r* was assessed 48h post-transfection by RT-qPCR using *igf-1r* specific primers and *Ubiquitin C (UBC)* was used as a gene housekeeping control for normalization of mRNA levels (E). The graphs show densitometry measurements of the average fold difference  $\pm$  SEM in IGF-1R protein expression (D) or average fold change difference  $\pm$  SEM in *igf-1r* mRNA expression (E), in FER-overexpressing cells compared with EV controls. Data are from  $n \geq 3$  independent experiments, a Two-way ANOVA with Bonferroni test was applied.

**F: Expression of IGF-1R WT and KD are both enhanced by FER.** Western blots were prepared with cell lysates from HEK293T cells (40 h post transfection) expressing either Empty Vector (pcDNA3; EV), IGF-1R/WT or Vector encoding IGF-1R/Kinase Dead (KD; K1003R mutant), as well as either empty vector (pSG5; EV) or FER. The blots were probed with anti-IGF-1R or anti-FER antibodies with  $\beta$  actin as a loading control. The graph represents densitometry measurements of average fold difference in IGF-1R protein expression  $\pm$  SEM in cells expressing EV, IGF-1R/WT or KD, together with EV or FER from four independent experiments. Two-way ANOVA with Bonferroni test was applied.

**G: FER kinase activity is not required for FER-mediated increased expression of IGF-1R.** 40 h post- transfection, HEK293T cells expressing empty vector (pcDNA3; EV), IGF-1R/WT or IGF-1R/KD and/or empty vector control for FER (pSG5; EV), FER or FER/KD, were lysed and immunoblotted for IGF-1R and FER expression. Densitometry measurements of mean  $\pm$  SEM average fold difference in IGF-1R protein expression from three independent experiments; One-way ANOVA with Bonferroni test was applied.

## Figure 2.

**FER promotes phosphorylation of WT and kinase-inactive IGF-1R and enhances signaling output.**

**A, B: Western blotting analysis of IGF-1R phosphorylation** in HEK293T (A) or R- (B) cells co-over-expressing: EV (-) or FER (+) with EV, IGF-1R/WT (WT) or IGF-1R/KD (KD). Cells were lysed 48 h after transfection and Western blots were prepared to assess levels of P-Y950, P-Y1131, P-Y1135/1136, and total IGF-1R. The levels of total FER were assessed as a control for transfection efficiency. Densitometry measurements of mean  $\pm$  SEM average fold difference in

specific P-Y site as indicated on the x-axis in the described above conditions based on at  $n \geq 3$  independent experiments; Two-way ANOVA with Bonferroni test.

**C: Western blotting analysis of IGF-1R phosphorylation** in HEK293T cells co-overexpressing: EV, FER or FER/KD with IGF-1R/WT (WT) or IGF-1R/KD (KD). At 48 h post transfection, cells were serum starved for 4 h, IGF-1 -stimulated (10 min; 10 ng/ml; +) and subsequently lysed for Western blots to assess levels of P-Y950, P-Y1131, P-Y1135/1136, and total IGF-1R. FER levels were assessed as a control for transfection efficiency.

**D: Western blotting analysis of IGF-1-mediated downstream signaling pathways** in HEK293T cells co-overexpressing: EV, FER or FER/KD with IGF-1R/WT (WT) or IGF-1R/KD (KD). At 48 h post transfection, cells were serum starved for 4 h prior to IGF-1 -stimulation (10 min; 10 ng/ml; +). Western blots were prepared to assess levels of P-SHC (Y239/Y240), P-FAK (Y397, Y925), P-SRC (Y416), and P-AKT (S473). The levels of total FER were assessed as a control for transfection efficiency. Densitometry measurements of mean  $\pm$  SEM average fold difference in specific P-Y proteins/total protein levels as indicated above the graph, based on  $n \geq 3$  independent experiments. Statistical analysis was performed using Two-way ANOVA with Bonferroni test.

### Figure 3.

#### **FER, IGF-1R and $\beta$ 1 integrin associate in adhesion complexes that enhance FER activity.**

**A-B. Co-localization of IGF1R with  $\beta$ 1 integrin and FER with  $\beta$ 1 integrin.** Confocal images of MCF-7 cells grown for 24 h on coverslips co-stained for FER (red) and IGF-1R (rabbit antibody, green; A),  $\beta$ 1 integrin (red) and IGF-1R (mouse antibody, green; upper panels, B) and FER (red) and  $\beta$ 1 integrin (green; lower panels, B) using antibodies described in methods. Co-localization is shown by the overlap of the fluorescent labels appearing in yellow. Cells were imaged using an Olympus Fluoview FV1000 confocal laser scanning microscope and Z-stacks were acquired and analysed using Fluoview Olympus software. At least two slices were acquired at different Z positions (Z1-Z2). Zoomed images (a, b) are presented in their respective Z-planes. Individual slices were 0.5  $\mu$ m thick. Scale represents 20  $\mu$ m. **C:** MDA-MB-231 were grown on coverslips coated with 5  $\mu$ g/cm<sup>2</sup> collagen I for 24 h and immunofluorescence staining was performed. IGF-1R (mouse, Millipore) and  $\beta$ 1-Integrin (rabbit, green) are shown in the upper panels and FER (mouse) and  $\beta$ 1-Integrin (rabbit, green) shown in the lower panels. A yellow

signal depicts areas of co-localization of the red and green fluorescent labels. The nuclei were stained with Hoechst (blue). Original 40x magnification, scale bars represent 200  $\mu\text{m}$ . **D: FER phosphorylation is enhanced by cell adhesion.** At 40 h post-plasmid DNA transfection, HEK293T cells expressing EV, IGF-1R/WT or IGF-1R/KD were serum starved for 4 h and stimulated with IGF-1 (10 min; 10 ng/ml;+), lysed and immunoblotted for P-Y402 FER/ FER. P-AKT and P-ERK1/2 were used as IGF-1 treatment controls. Densitometry measurements of mean +/- SEM average fold difference in P-Y402 FER in the above conditions based on 3 independent experiments; Two-way ANOVA with Bonferroni test. **E, F:** Western blotting analysis of EV, FER/WT or FER/KD overexpressing HEK293T cells. 48 h post- DNA transfection, cells were lysed and immunoblotted for the indicated phospho- and total protein levels. Densitometry measurements of mean +/- SEM average fold difference in specific P-Y proteins/total protein levels as indicated on the y-axis in the described above conditions based on  $n \geq 3$  independent experiments. One-way ANOVA with Bonferroni test was applied

#### **Figure 4**

#### **Suppression of FER with siRNA suppresses IGF-1R activity and cell proliferation, but variably affects migratory potential**

**A: Suppression of FER with siRNAs affects IGF-1R levels:** Protein expression of the indicated proteins was analyzed by immunoblotting in control (siNEG) cells and cells treated with 2 different FER siRNAs (siFER2 or 3), 48 h post-transfection. Graphs show densitometry measurements of mean fold difference +/- SEM of IGF-1R expression in siFER-transfected cells compared with siNEG controls, based on at least  $n=3$  independent experiments; Statistical analysis was performed using Two-way ANOVA with Bonferroni test. **B: Western blot analysis of IGF-1R downstream signaling in cells with FER suppressed:** At 48 h post-transfection with siNEG or FER siRNAs, MCF-7 and MDA-MB-231 cells were serum starved for 4 h prior to stimulation with IGF-1 (10 ng/ml), for indicated times. Cell lysates were assessed by SDS-PAGE and immunoblotting for expression of FER, IGF-1R, P-AKT and P-ERK and non-phospho controls. Graphs of mean fold difference +/- SEM of P-ERK and P-AKT expression are shown in the graphs, quantified by densitometry from 3 independent experiments. Statistical significance was analyzed by Two-way ANOVA with Bonferroni test. **C. FER suppression causes decreased cell proliferation:** 24 h post-transfection with siNEG or FER siRNAs, cells were plated in triplicate at the same cell number and fixed and stained with crystal

violet every 24 h for a further 96 h. Staining intensity at each timepoint was analyzed using an Odyssey scanner and densitometric measurements from 3 separate experiments +/- SEM are shown. Statistical significance was determined using a Two-way ANOVA with Bonferroni test.

**D: FER siRNA 2 and 3 have variable effects on migration:** 24 h post-transfection, siNEG, siFER2 and siFER3- treated MDA-MB-231 cells were seeded onto the upper part of a transwell chamber in serum-free medium, and allowed to migrate towards serum for 24h. Cells that had migrated to the underside of the transwell membrane ('Membrane'), and cells that had migrated through the membrane entirely and attached to the bottom of the well ('Through migration') were fixed and stained with crystal violet and measured using an Odyssey scanner.

Quantification of migration was first normalized to cell proliferation (shown in graph on right), for each cell type. Data is shown as percentage migration, of membrane or 'through' migration, with siNEG total cell migration set as 100%. Images of the transwell membrane- and 'through'-migrated cells are shown, n=1. **E: siRNA3-transfected cells have decreased cell adhesion to fibronectin, whereas FER siRNA2 does not affect adhesion:** MDA-MB-231 cells were plated

onto fibronectin (FN; 5µg/ml) or collagen I (Col; 10µg/ml) -coated wells, 48 h post-transfection with siNEG or siFER2 or 3. Cells were fixed and stained with crystal violet 20, 40 or 60 min after plating. Quantification of adherent cells was measured using Odyssey scanning and densitometry. Data is presented as fold change of adhesion of siNEG cells, from 3 independent experiments, statistical analysis was performed using the Student's t-test.

## **Figure 5.**

**Cell adhesion is required for FER enhanced IGF-1R activity.**

**A, B: Immunofluorescence of MDA-MB-231 with suppressed FER.** MDA-MB-231 were plated onto coverslips coated with 5 µg/cm<sup>2</sup> collagen, 24 post-transfection with siNEG or siFER2 or 3. Cells were allowed to attach for 24 h, fixed and stained with IGF-1R, β1-Integrin, and FER. **A:** MDA-MB-231 with suppressed FER showing less co-localization of IGF-1R (red) with β1-Integrin (green) in adhesion complexes indicated by a reduced yellow signal illustrated in siNEG merged image compared with merged images of siFER2 and siFER3. **B:** MDA-MB-231 cells transfected with siFER2 or 3 show reduced FER staining (red), whereas β 1-integrin (green) levels are similar. Images in A and B also illustrate differences in cell morphology between cells transfected with siFER2 (more spread) and siFER3 (elongated). Images were taken in 40x and

the scale bars represent 200  $\mu\text{m}$ . **C: Immunofluorescence shows cortactin and IGF-1R co-localization in MCF-7 cells.**

MCF-7 cells grown on coverslips for 24 h were fixed and stained with combinations of anti-IGF-1R (rabbit/mouse; green) and anti-cortactin (mouse; red). Slides were imaged Olympus Fluoview FV1000 confocal laser scanning microscope. Z-stacks were acquired and analysed using Fluoview Olympus software. At least two slices were acquired at different Z positions (Z1-Z2). Zoomed images (a, b, c) are presented in their respective Z-planes. Individual slices were 0.5  $\mu\text{m}$  thick. Scale represents 20  $\mu\text{m}$ .

**D, E: Suppression of cortactin in MCF-7 cells reduces IGF-1R levels.** Total lysates of MCF-7 were analyzed 48 h post-transfection with negative control siRNA (siNEG) or cortactin siRNA (siCTN) for IGF-1R and cortactin expression. **E:** MDA-MB-231 cells were analyzed 24 h post-transfection with negative control siRNA (siNEG) or cortactin siRNA (siCTN). Cells were immediately either cultured in the presence of DMSO (CTRL) or Bortezomib (PROTEAS-i; 30 nM) for 24 h. Expression of IGF-1R, FER and ubiquitin as a control for proteasome inhibition, were analyzed by Western blotting.

**F: Cell adhesion is required for FER-mediated IGF-1R phosphorylation.** Western blotting analysis of IGF-1R phosphorylation and FER signaling in HEK293T cells co-overexpressing: EV, FER/WT, or FER/KD with IGF-1R/WT (left panels) or IGF-1R/KD (right panels) as indicated. 48 h post-transfection, cells were transferred into suspension culture for 2 h, subsequently lysed and immunoblotted to assess levels of P-IGF-1R (Y1131, Y1135/6), IGF-1R, P-SHC (Y239/Y240) and P-FAK (Y397) as a control of the loss of adhesion signaling. The levels of total FER were assessed as a control for transfection efficiency. The experiments were performed three times with similar results while the graph represents quantification of Y1131 and Y1135/1136 (an average of two of these experiments).

**G: Loss of adhesion signaling decreases autophosphorylation on FER.** IGF-1R/WT-expressing HEK293T cells were treated as described above. A reduced level of P-Y402 FER was observed when cells were in suspension. P-Y397 FAK was used as a control for the loss of adhesion signal.

**Figure 6:****High FER expression in mesenchymal breast cancer negatively correlates with relapse-free survival. Pharmacological inhibition of FER kinase abolishes its signaling.**

**A:** Kaplan Meier plots were drawn using data accessed through KM-plotter, a publicly accessible interface for TCGA survival data. All data sets were assayed using probe ID: 206412. P-value, hazard ratio (HR) and median survival were calculated and are displayed. **B:** RNA-Seq analysis of FER mRNA expression compared in low and highly migratory or luminal, basal A, and mesenchymal (basal B) breast cancer cell lines (n=78), extracted from Marcotte *et al.* (2016). FER mRNA expression is plotted on a log<sub>2</sub> scale. **C:** Table representing *in situ* analysis of correlation of FER and expression of several mesenchymal genes in breast cancer cell lines (n=82), extracted from Marcotte *et al.* 2016. **D:** Western blotting analysis of FER protein expression and phosphorylation of SHC in a panel of breast cancer cell lines. **E:** Western blotting analysis of effects of FER-i (AP26113) on IGF-1R/WT and EV or FER-co-expressing HEK293T cells. At 48 h post transfection cells were cultured with AP26113 (0-500 nM) for 2 h, subsequently lysed and immunoblotted for the indicated phospho- and total protein levels. FER immunoblot was included as an overexpression control. **F:** Western blotting analysis of effects of FER-i (AP26113) on endogenous FER and signaling in HS578T cells. Cells were treated for 2 h with 0-2  $\mu$ M, subsequently lysed and immunoblotted for the indicated phospho- and total protein levels. **G, H:** Effects of FER-i on HS578T cell migration were assessed by wound healing assays as described in Methods. Cells were pre-treated with AP26113 prior to wounding and maintained in medium containing 0.5 $\mu$ M inhibitor for 15 h post-wounding. Plates were photographed with under phase contrast at 10x magnification and the image represents one of three independent experiments with similar results. **H:** After 15 h of exposure to AP26113 cells were lysed and Western blots prepared to assess levels of Y402 FER, total FER and IGF-1R.

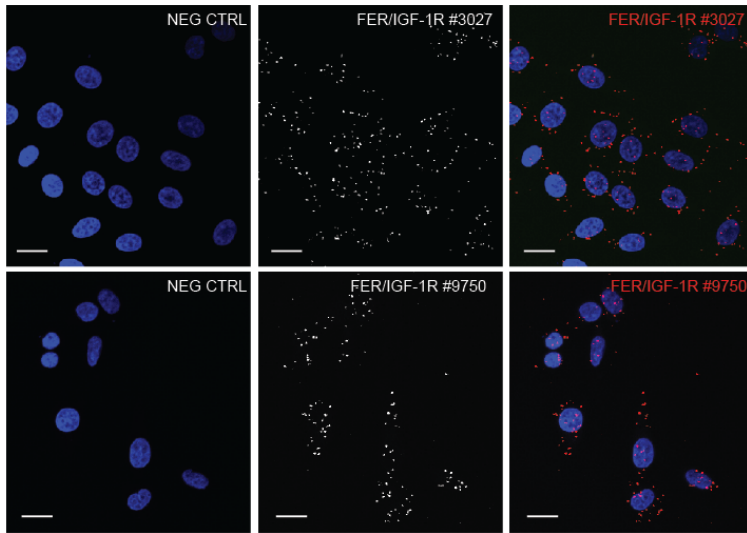
**Figure 7.****Schematic representing the role of FER in potentiation of cooperative signaling between IGF-1R/ $\beta$ 1 Integrin at sites of cell adhesion.**

We propose that the non-receptor tyrosine kinase FER is an important signaling node in cooperative signaling between the IGF-1R and cell adhesion signaling. FER-IGF-1R axis has a direct effect on IGF-1R steady state levels, its phosphorylation and signaling output.

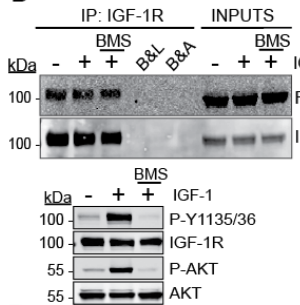
(CTN – cortactin).

Figure 1

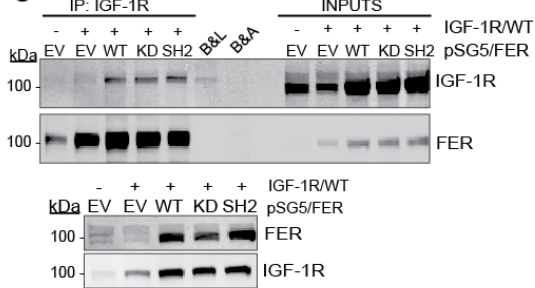
A



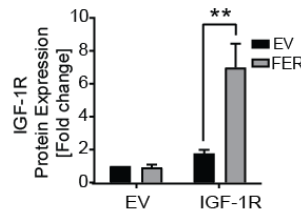
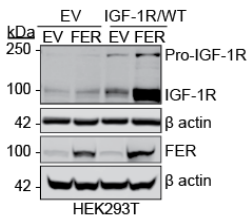
B



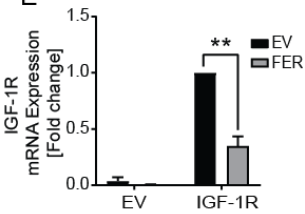
C



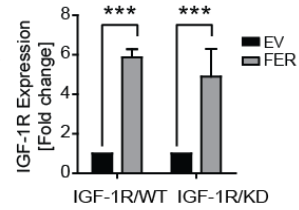
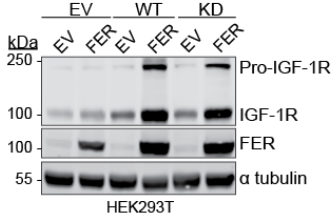
D



E



F



G

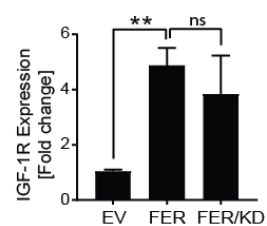
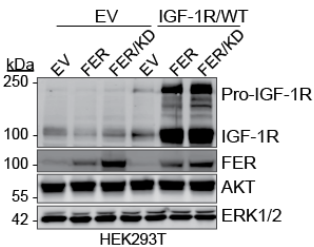


Figure 2

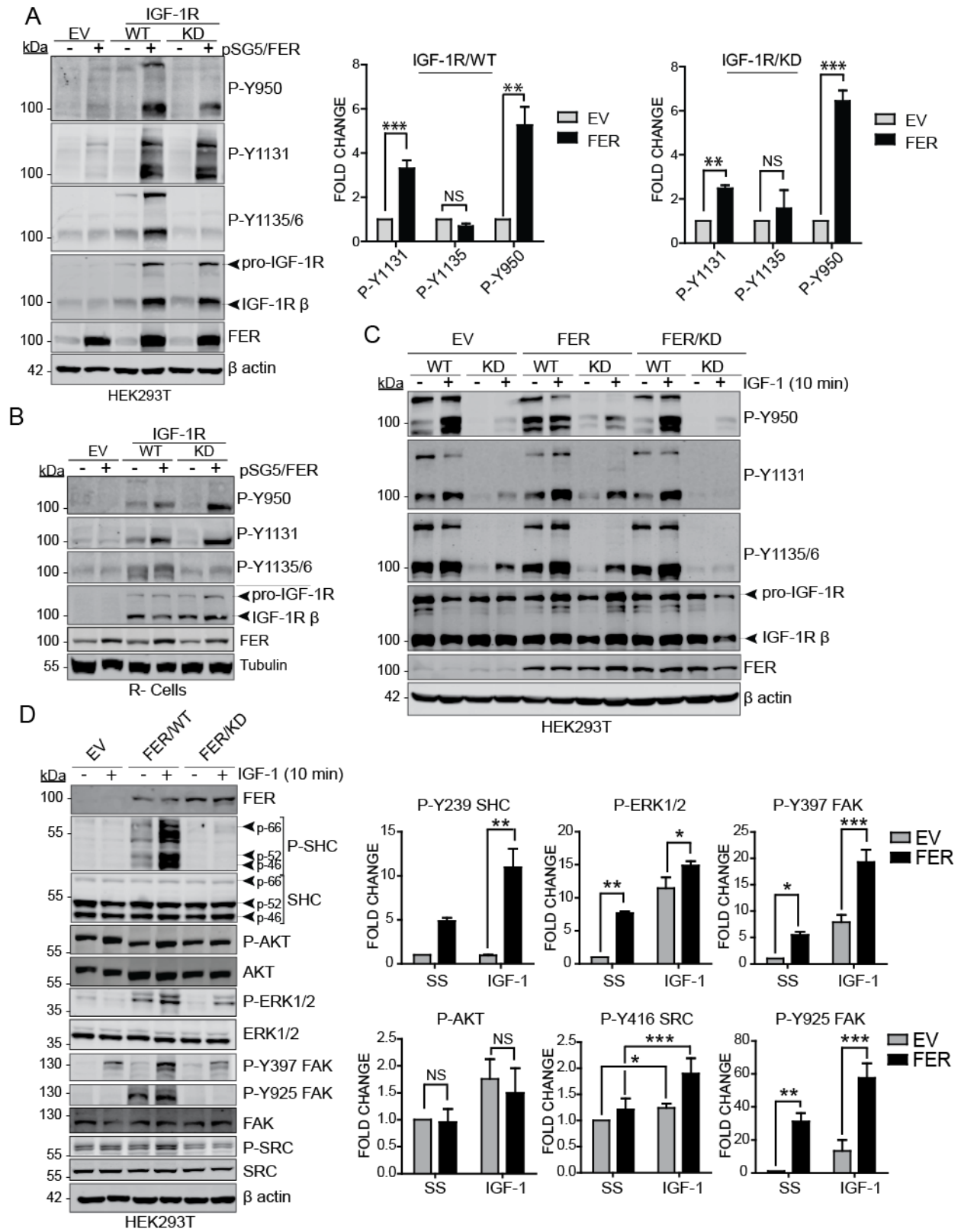


Figure 3

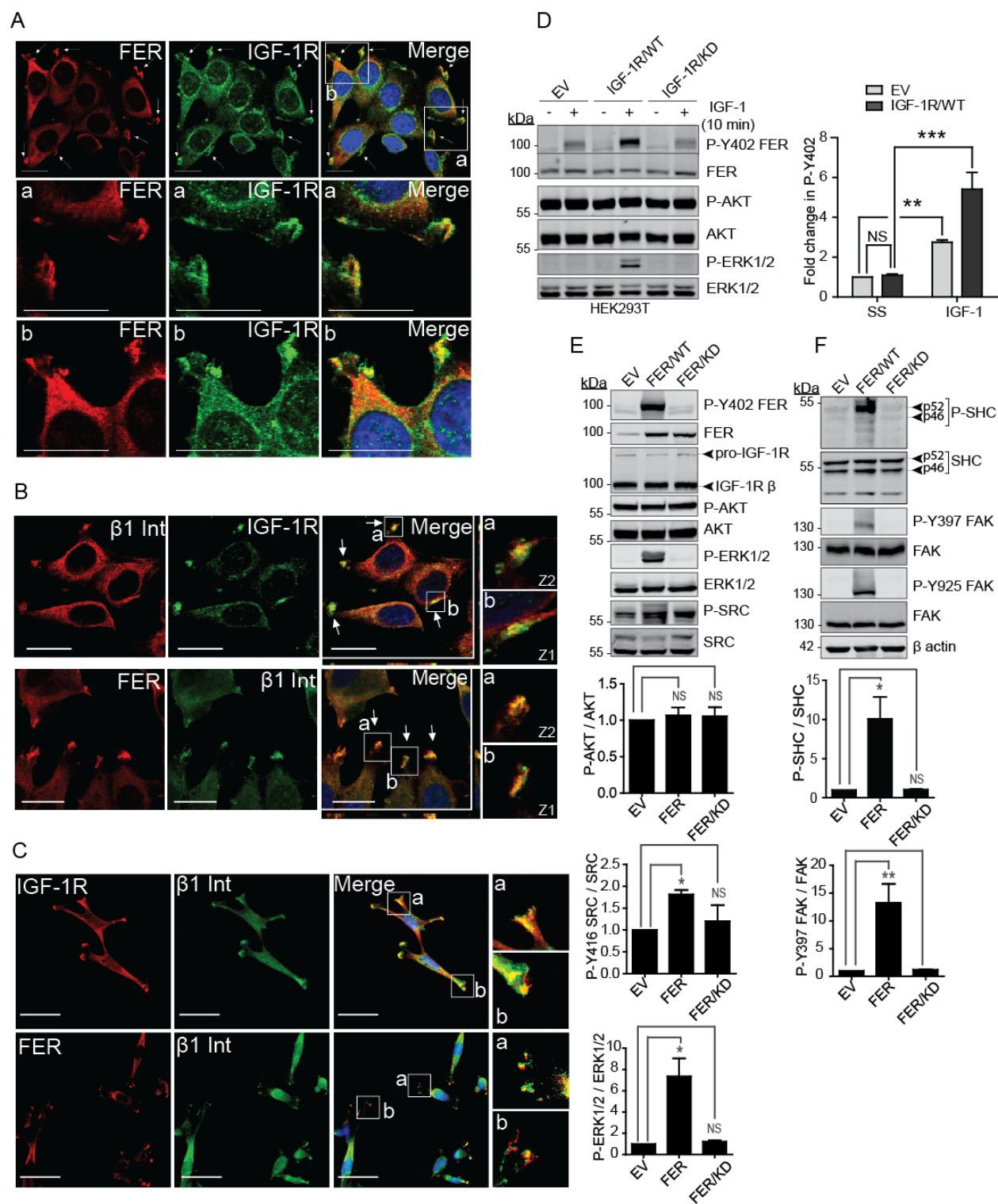


Figure 4

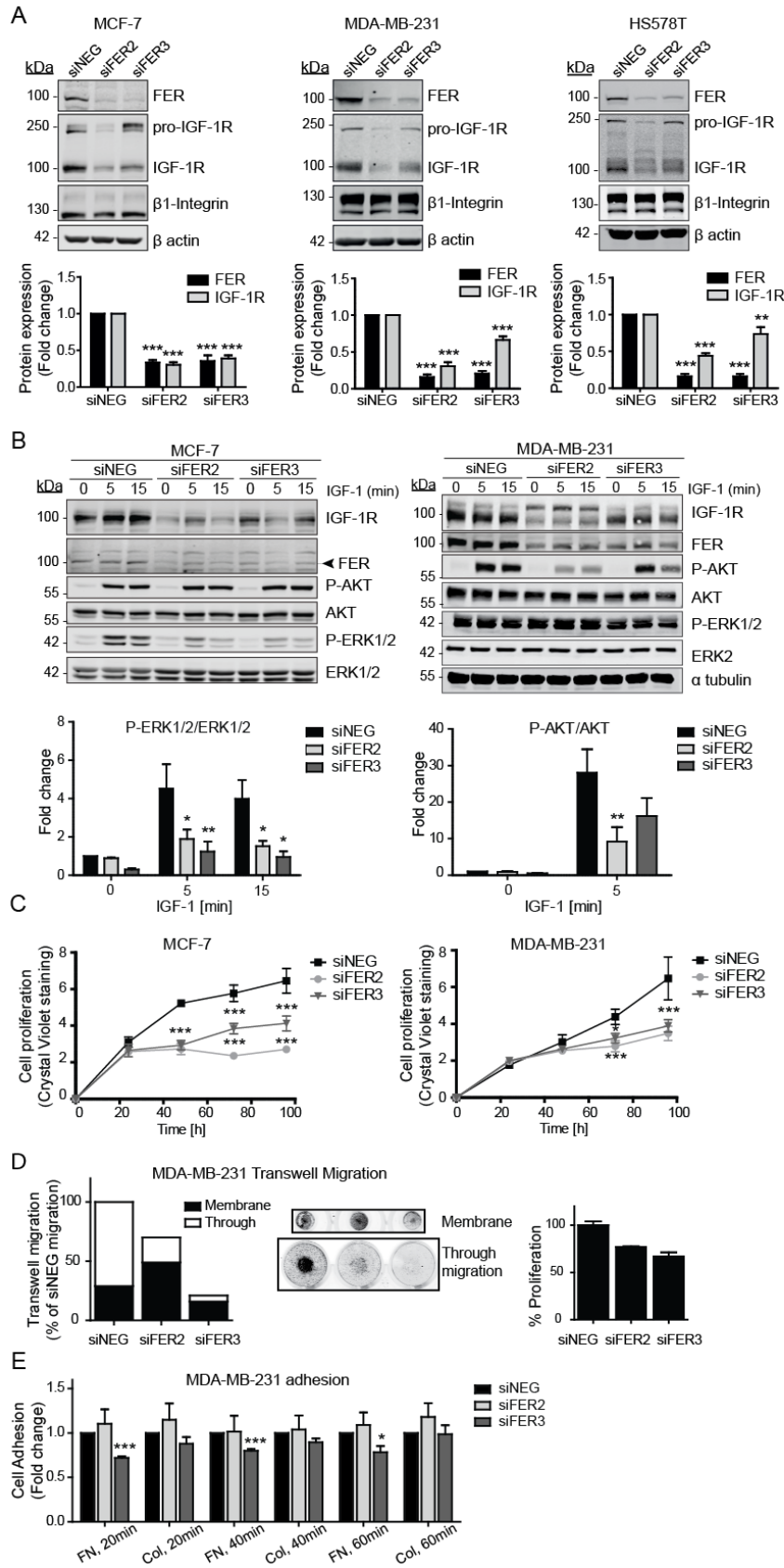


Figure 5

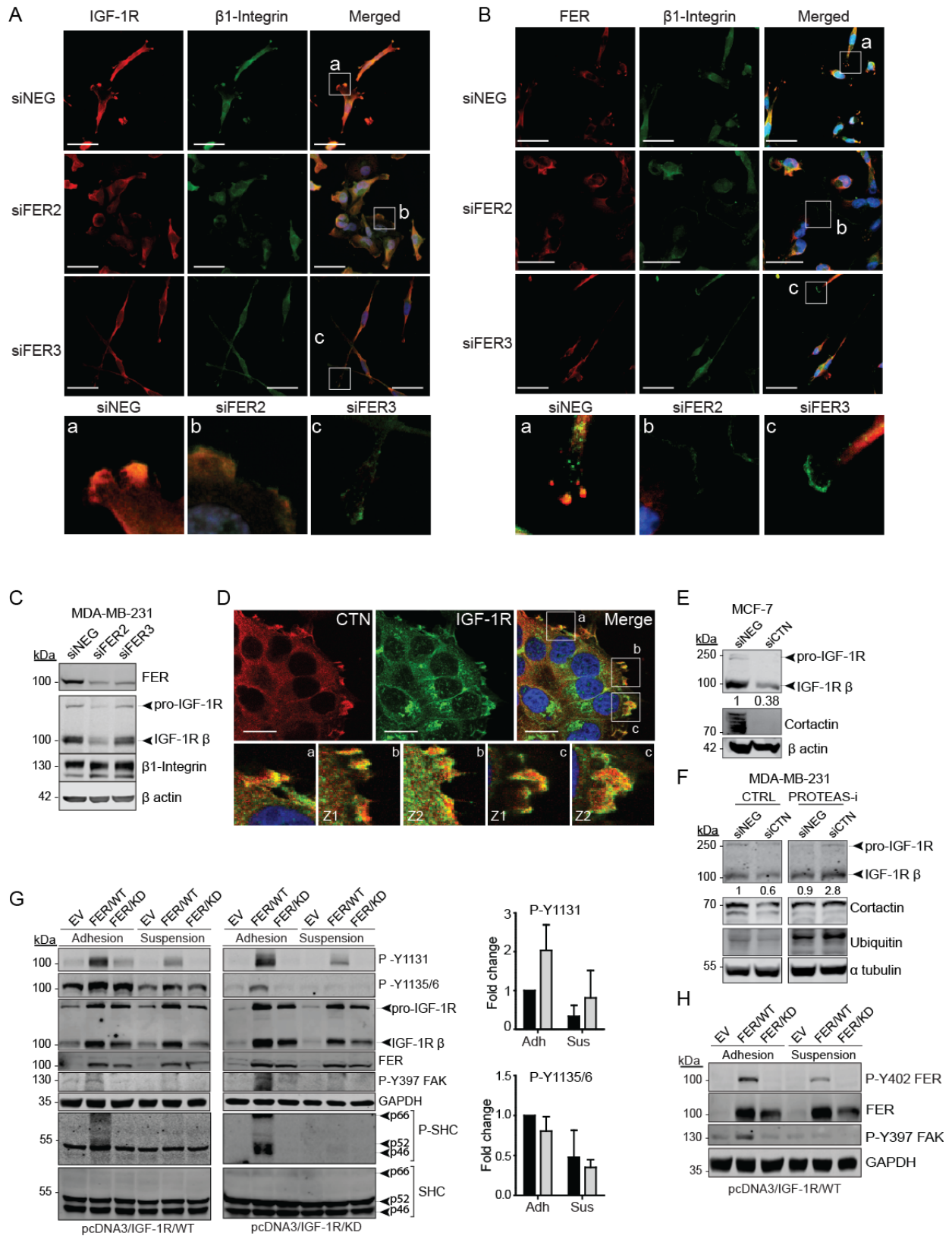


Figure 6.

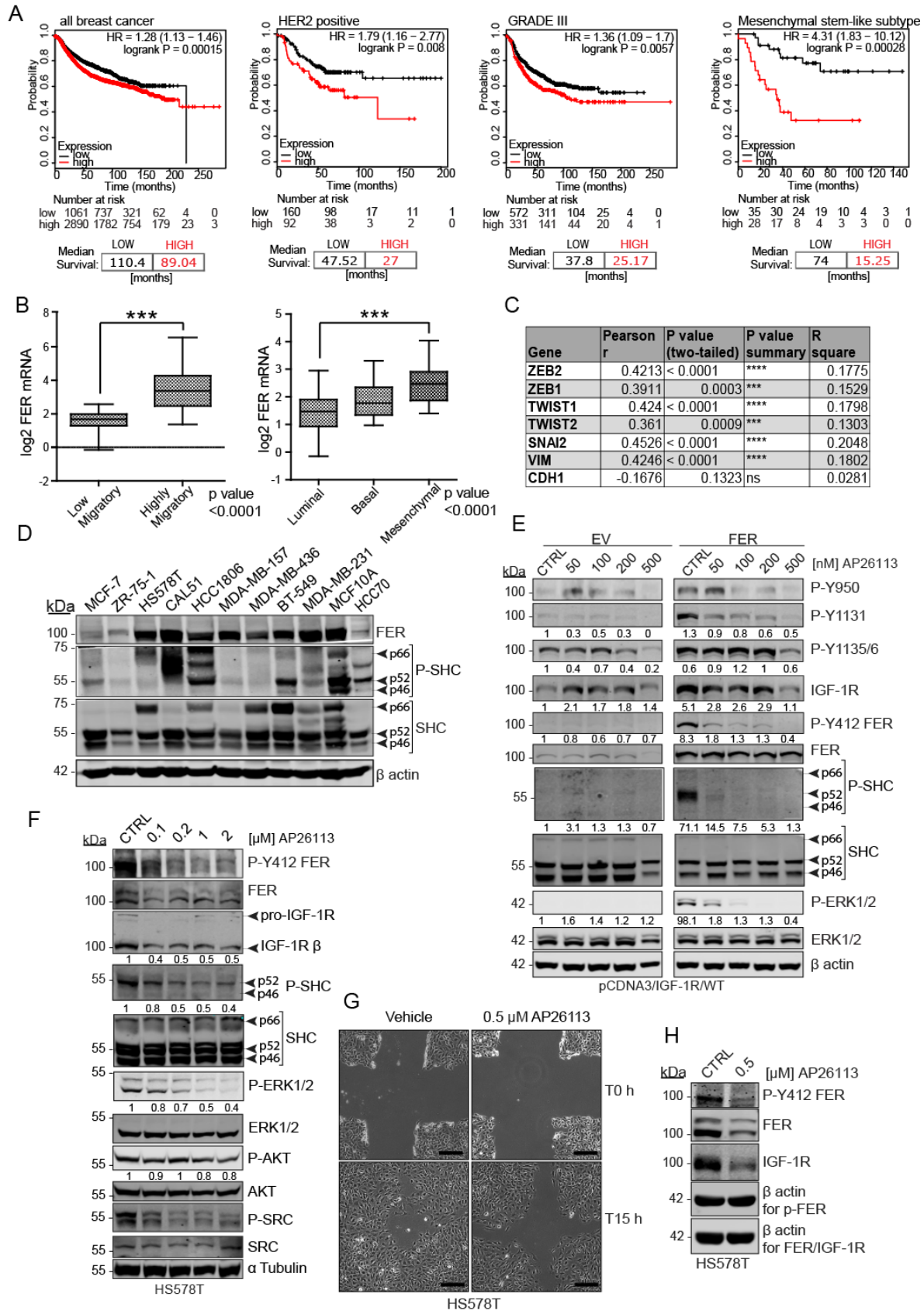


Figure 7.

